

REMARKS

Claim Status

Claims 1-7, 13, 15 and 18-20 have been cancelled without prejudice.

Previously withdrawn claims 14 and 17 have been amended to improve clarity as well as to update the dependency.

Claim 21 has been amended to correct a clerical error, i.e., changing the second step “(b)” to “(c)”.

Claim 24 has been amended to replace the phrase “another amino acid” with “a serine”. Support for such amendment can be found in claim 7.

New claims 26 and 27 have been added, which further characterize the pharmaceutical composition of claim 25. Support for these new claims can be found in claims 19-20.

Applicants respectfully submit that the foregoing amendments do not introduce any new matter to the original application as filed. With the present amendments, claims 14, 16-17 and 21-27 are pending. It is noted that new claims 26 and 27 fall within the scope of the previously elected invention. As such, they should be joined with claims 21-25 for further examination.

It is further noted that withdrawn claims 14 and 16-17 are patentably related to the elected claims as product and process of use. Applicants respectfully request that the withdrawn process of use claims be rejoined with the elected product claims and fully examined for patentability upon the allowance of the product claims. *See* MPEP §821.04(b).

Claim Rejections - 35 U.S.C. § 103(a)

Claims 1, 2, 6, 13 and 18-20 remain rejected and previously added claims 21, 23 and 25 stand rejected under 35 U.S.C. §103(a) as allegedly being unpatentable over Smith et al. (WO 9847531; “Smith” hereafter) in view of Hsu et al. (Transplantation. 1999 Aug 27; 68(4): 545-54; “Hsu” hereafter), Holliger et al. (U.S. Pat. No. 5,837,242; “Holliger” hereafter) and Chapman et al. (Nat. Biotechnol. 1999 Aug; 17(8): 780-3; “Chapman” hereafter). In response, Applicants respectfully traverse this rejection.

It is first noted that claims 1, 2, 6, 13 and 18-20 have been cancelled without prejudice. New claims 26 and 27 have been added, dependent upon claim 25. Applicants extend the present rejection to newly added claims 26 and 27.

Teachings of present invention and cited references

The present invention is directed to a bivalent, non-covalent anti-CD3 diabody. A representative example of the claimed diabody is scFv6 diabody, which is a dimer and has a molecular weight of about 60 kDa (*see* page 21, last three lines and page 22, lines 1-2 of the instant specification, as well as Fig. 1). This structure is devoid of constant domains and consists of two polypeptide chains which are associated with one another to form two CD3 binding sites.

Smith discloses F(ab')₂, which are a large portion of a whole antibody and have a distinct structure from that of the diabody of the present invention. In particular, F(ab')₂ are coupled by a hinge-joint which gives flexibility to the antigen binding domains to orientate towards the respective epitopes on CD3 molecules. Additionally, Smith does not provide any suggestion to make a diabody devoid of constant domains.

Hsu reports that a Fc receptor non-binding anti-CD3 antibody is not associated with serious side-effects and that a significant cytokine release occurs when the Fc domain of a human anti-CD3 antibody is able to bind to Fc receptors on chimpanzee cells. Hsu does not suggest making an antibody devoid of constant domains.

Holliger discloses use of bivalent diabodies for cross-linking CD3 to activate T cells (Col. 22, lines 15-16 thereof). Holliger does not teach diabodies that suppress immune reaction.

Chapman discloses antibody; however, it does not teach or suggest diabody.

The above references, along or combined, do not render the instant claims obvious for the reasons stated below.

No motivation to combine prior art references in achieving immunosuppression effect

Smith teaches that the mechanism of immunosuppression by anti-CD3 antibodies is complex (page 17, line 1 thereof) and that various anti-CD3 antibodies may suppress T cell responses by distinct mechanisms (page 17, lines 9-10 thereof). The findings of Smith regarding mutated IgG antibodies are therefore not necessarily indicative of any other CD3-binding molecules. Smith reports, for example, that the mutated IgG antibody appeared to immunomodulate the Th1/Th2 cytokine balance in favour of Th2, which Smith attributed to partial T cell signalling. This also appeared to result in significant proliferation of Th2 cells (Fig. 25B thereof).

Smith describes IgG antibodies having a Y-shaped structure and F(ab')₂ fragments having a V-shaped structure. In both instances the geometry and flexibility of the antibody permits the efficient binding of the two arms to more than one antigen on the cell surface thus increasing avidity. The F(ab')₂ fragments still have the hinge region, thus retaining the geometry and flexibility of the full length antibody. Multivalent binding also enhances the cross-linking of antigens on the cell surface. This can lead to the inhibition or stimulation of the signalling pathway associated with a particular antigen.

Holliger discloses diabodies that have a rigid structure and a back to back position of the binding sites (Col. 15, l. 49-58) and that the lack of flexibility is unlikely to compromise the cross-linking of two soluble antigens, or of a cell surface antigen and a soluble antigen (Col. 16, l. 58-62). Holliger further teaches cross-linking the CD3 antigen so as to activate T cells (Col. 22, lines 15-16). It is noted that Holliger always assumes that the T cells will be activated through the action of the diabodies.

Holliger discloses the efficacy of the diabody format for connecting two cells. There have been no examples shown, however, of diabodies comprising an anti CD3 binding site being able to bind with both binding sites simultaneously to the same cell surface. Indeed, the efficacy of T-cell activation by cross-linking a diabody bound at one end to CD3 teaches away from the likelihood that the T cells would be down-regulated. There appears to be no essential difference between cross-linking CD3 on the T cell surface by a diabody that binds to CD3 on a T-cell at one end and that binds to either a B-lymphocyte or another T-cell at the other end. It would certainly not have been surprising in view of the above facts if a stronger T cell activation had been obtained when the CD3 molecules were cross-linked by T-cell bridging rather than T-cell-B-lymphocyte bridging.

Therefore, Holliger does not indicate that an anti-CD3 diabody may act as an immunosuppressant. To the contrary, Holliger only teaches that T cells will be activated by the diabodies. Considering that Smith emphasizes the modulation of CD3 is highly complex and different antibodies have different mechanisms of action, and that not any immunosuppressive activity was indicated for diabodies, one skilled in the art would not have been motivated to select an anti-CD3 diabody as an alternative for F(ab')₂ fragments as an immunosuppressant.

At page 3 of the present Office Action, the Examiner argues that "[o]ne of skill in the art

would have been motivated to make an anti-CD3 diabody in particular because, unlike the bivalent anti-CD3 $F(ab')_2$, the bivalent anti-CD3 diabody does not run the risk of being contaminated with intact antibodies. Furthermore, given the large-scale cost efficient production is possible with Fab', Fv and scFv according to Chapman, one of ordinary skill in the art, filtered through their knowledge of the art, would readily surmise that large-scale cost efficient production of a diabody would also be reasonable, in contrast to the teachings of Smith regarding the difficulty of producing large quantities of $F(ab')_2$ fragments". Applicants cannot agree with the Examiner's position for the reasons stated below.

Methods for the high yield production of $F(ab')_2$ fragments have been described by Holliger (e.g. Col. 13, l. 27-28; Col. 13, l. 52 – Col. 14, l. 10) and Chapman. These references clearly teach that the production of homogeneous recombinant products in *E.coli* is rapid, economical and avoids any potential contamination with the full length antibody. One skilled in the art would readily realize that the drawbacks of $F(ab')_2$ preparation such as small quantities and contamination with full length mAb reported by Smith can be overcome by recombinant production of $F(ab')_2$ in bacteria as taught by Holliger and Chapman.

That is, Holliger and Chapman provide obvious solution to the problems reported by Smith, which solution involves producing recombinant $F(ab')_2$ in bacteria. Such solution does not require changing the type of antibody from $F(ab')_2$ to a diabody. That is, Holliger and Chapman do not suggest using a diabody as an alternative to anti-CD3 $F(ab')_2$ fragments to solve the yield problems reported by Smith. Considering that Smith teaches that $F(ab')_2$ fragments were as efficacious as whole antibodies and that Holliger and Chapman teach how the drawbacks associated with $F(ab')_2$ reported by Smith can be overcome by cost-effective large-scale production in bacteria, one skilled in the art would not have been motivated to replace the $F(ab')_2$ fragment with a quite different antibody structure such that of a diabody for which the suitability for immunosuppression was neither known nor indicated prior to the filing of the present application. In fact, there is no incentive for such replacement.

Additionally, as Holliger teaches that a diabody activates T cell proliferation instead of suppressing the proliferation, one skilled in the art would not have replaced a highly efficient $F(ab')_2$ fragment with a diabody as an immunosuppressant as Holliger teaches opposite effect of a diabody.

Unexpected and superior immunosuppression effect of diabody

Applicants herewith submit a Rule 132 declaration by Dr. Melvin Little, one of the co-inventors of the present application, stating the superior and unexpected immunosuppression property of the instantly claimed diabody. Therein, the instantly claimed diabody, a TandAb (tandem diabody) antibody and a full length OKT3 antibody were compared in terms of the induced T cell proliferation and the modulation of T cell receptor.

The TandAb (tandem diabody) was described in Kipriyanov et al. (J. Mol. Biol. (1999) 293, 41-56; copy enclosed for the Examiner's consideration). This dimeric antibody structure is composed of two polypeptide chains containing only variable domains linked by short peptide linkers which, similar to the instantly claimed diabodies, associate with one another to form the antigen binding molecule. Each of the polypeptide chains contains four variable domains and the TandAb is tetravalent. The TandAb molecule is structurally similar to the instantly claimed diabody as the former can be considered as two diabody molecules joined with one another. Moreover, both the instantly claimed diabody and the TandAb are devoid of any constant domains, which is of particular relevance in the present case. Therefore, the TandAb is considered to represent a closest prior art to the instantly claimed diabody.

While all three different kinds of antibodies (OKT3, diabody and TandAb) showed very similar T cell receptor down modulating activity (*see* Fig. 2 of the declaration), OKT3 and TandAb induced significant proliferation of PBMC, but the instantly claimed diabody induced no significant proliferation (*see* Fig. 1 of the declaration).

Since both the instantly claimed diabody and the comparative TandAb comprise the same anti-CD3 domains and are devoid of all constant domains, the result that the TandAb induced a significant proliferation while the instantly claimed diabody did not clearly suggests that lacking an FcR binding region does not automatically result in an avoidance of T cell proliferation. This is also in accordance with the "reduced" T cell activation of F(ab')₂ fragments taught by Smith. Therefore, it was all the more surprising that the instantly claimed anti-CD3 diabody did not induce any T cell proliferation at all.

Smith teaches that F(ab')₂ fragments lacking the Fc domain exhibited significantly reduced T cell activation and fewer side effects (page 50, 1st full paragraph). This is confirmed by the TandAb which lacks an Fc domain and induced a significant lower cell proliferation than

the OKT3 (*see* Fig. 1 of the declaration). However, it could not be expected that a cell proliferation can be avoided by the instantly claimed diabody. Such property of extremely low immunogenicity of the instantly claimed diabody is a marked improvement over the TandAb or the OKT3, which provides the practical advantage of allowing administration of the instantly claimed diabody at higher dosages and repeated times.

In view of the foregoing amendments and remarks, Applicants respectfully submit that the cited references do not render the instant claims obvious. As such, the rejection under 35 U.S.C. §103(a) should be withdrawn.

Claims 5 and 7 remain rejected and previously added claims 22 and 24 stand rejected under 35 U.S.C. §103(a) as allegedly being unpatentable over Smith, in view of Hsu, Holliger and Chapman as applied to claims 1, 2, 6, 13, 18-20, 21, 23 and 25 above, and further in view of Kipriyanov et al. (Protein Eng. 1997 Apr; 10(4):445-53; “Kipriyanov” hereafter). In response, Applicants respectfully traverse this rejection.

It is first noted that claims 1, 2, 6, 13 and 18-20 have been cancelled without prejudice.

As discussed above, Smith, Hsu, Holliger and Chapman, alone or combined, do not disclose or suggest an anti-CD3 diabody according to the present invention.

Kipriyanov does not disclose or suggest that an OKT3 scFv shows an immunosuppressive effect. Therefore, the addition of Kipriyanov does not cure the deficiency of Smith, Hsu, Holliger and Chapman as discussed above. Thus, one skilled in the art would not have been motivated by Kipriyanov to use the specific linker of claim 22 or to use the modified domain of claim 24 to make an anti-CD3 diabody.

In view of the foregoing amendments and remarks, Applicants respectfully submit that the cited references do not render the instant claims obvious. As such, the rejection under 35 U.S.C. §103(a) should be withdrawn.

Claim Rejection - 35 U.S.C. § 112, 1st Paragraph (Enablement)

Claim 24 stands rejected under 35 U.S.C. §112, 1st paragraph, as allegedly failing to comply with enablement requirement. In response, Applicants respectfully traverse this rejection.

Claim 24 has been amended to recite that a cysteine at position H100A is changed to a serine. The enablement for such amended claim has been acknowledged by the Examiner. *See* page 5 of the present Office Action. As such, Applicants respectfully request that the rejection of claim 24 under 35 U.S.C. § 112, 1st paragraph, be withdrawn.

Respectfully submitted,

/j. wendy davis/

Date: January 7, 2010

J. Wendy Davis, Ph.D. (Reg. No. 46,393)
Viola T. Kung, Ph.D. (Reg. No. 41,131)

HOWREY LLP
2941 Fairview Park Drive, Box 7
Falls Church, VA 22042
Tel: (650) 798-3570
Fax: (650) 798-3600

Bispecific Tandem Diabody for Tumor Therapy with Improved Antigen Binding and Pharmacokinetics

Sergey M. Kipriyanov^{1*}, Gerhard Moldenhauer², Jochen Schuhmacher³
Björn Cochlovius¹, Claus-Wilhelm Von der Lieth⁴, E. Ronald Matys³
and Melvyn Little¹

¹Recombinant Antibody
Research Group (D0500)

²Department of Molecular
Immunology

³Department of Diagnostic and
Therapeutic Radiology and

⁴Department of Spectroscopy
German Cancer Research
Center (DKFZ), Im
Neuenheimer Feld 280
D-69120, Heidelberg, Germany

To increase the valency, stability and therapeutic potential of bispecific antibodies, we designed a novel recombinant molecule that is bispecific and tetravalent. It was constructed by linking four antibody variable domains (V_H and V_L) with specificities for human CD3 (T cell antigen) or CD19 (B cell marker) into a single chain construct. After expression in *Escherichia coli*, intramolecularly folded bivalent bispecific antibodies with a mass of 57 kDa (single chain diabodies) and tetravalent bispecific dimers with a molecular mass of 114 kDa (tandem diabodies) could be isolated from the soluble periplasmic extracts. The relative amount of tandem diabodies proved to be dependent on the length of the linker in the middle of the chain and bacterial growth conditions. Compared to a previously constructed heterodimeric CD3 \times CD19 diabody, the tandem diabodies exhibited a higher apparent affinity and slower dissociation from both CD3⁺ and CD19⁺ cells. They were also more effective than diabodies in inducing T cell proliferation in the presence of tumor cells and in inducing the lysis of CD19⁺ cells in the presence of activated human PBL. Incubated in human serum at 37°C, the tandem diabody retained 90% of its antigen binding activity after 24 hours and 40% after one week. *In vivo* experiments indicated a higher stability and longer blood retention of tandem diabodies compared to single chain Fv fragments and diabodies, properties that are particularly important for potential clinical applications.

© 1999 Academic Press

Keywords: bispecific diabody; tandem diabody; domain swapping; human CD19; human CD3

*Corresponding author

Introduction

Bispecific antibodies (BsAb) provide an effective means of retargeting cytotoxic effector cells against tumor cells (Fanger *et al.*, 1992). They have mainly been produced using murine hybrid hybridomas (Bohlen *et al.*, 1993) or by chemical cross-linking (Brennan *et al.*, 1985; Glennie *et al.*, 1987). However, the immunogenicity of BsAb derived from rodent monoclonal antibodies is a major drawback for clinical use (Khazaeli *et al.*, 1994). They are also dif-

ficult to produce and purify in large quantities. Recent advances in recombinant antibody technology have provided several alternative methods for constructing and producing BsAb molecules (Carter *et al.*, 1995; Plückthun & Pack, 1997). For example, single chain Fv (scFv) fragments have been genetically fused with adhesive polypeptides (de Kruif & Logtenberg, 1996) or protein domains (Müller *et al.*, 1998c) to facilitate the formation of heterodimers. The genetic engineering of scFv-scFv tandems linked with a third polypeptide linker has also been carried out in several laboratories (Gruber *et al.*, 1994; Kurucz *et al.*, 1995). A bispecific diabody was obtained by the non-covalent association of two single chain fusion products consisting of the V_H domain from one antibody connected by a short linker to the V_L domain of another antibody (Holliger *et al.*, 1993, 1996). The two antigen binding domains have been shown by

Abbreviations used: scFv, single chain Fv; sc-diabody, single chain diabody; LL, long linker; SL, short linker; Tandab, tandem diabody; BsAb, bispecific antibody; TCR, T cell receptor; IMAC, immobilized metal affinity chromatography; AUC, area under the curves.

E-mail address of the corresponding author:
s.kipriyanov@dkfz-heidelberg.de

crystallographic analysis to be on opposite sides of the diabody such that they are able to cross-link two cells (Perisic *et al.*, 1994). In contrast to native antibodies, all of the above mentioned bispecific molecules have only one binding domain for each specificity. However, bivalent binding is an important means of increasing the functional affinity and possibly the selectivity for particular cell types carrying densely clustered antigens.

We recently described the construction and characterization of a bispecific diabody with dual specificity for both the human B cell antigen CD19 and ϵ chain of the CD3/T cell receptor (TCR) complex designed for the treatment of minimal residual disease in patients with leukemias and malignant lymphomas (Kipriyanov *et al.*, 1998). The CD19 antigen is expressed on virtually all B-lineage malignancies from acute lymphoblastic leukemia (ALL) to non-Hodgkin's lymphoma (NHL) (Uckun & Ledbetter, 1988). Moreover, it is not shed and is absent from hemopoietic stem cells, plasma cells, T cells and other tissues. Bispecific diabodies appear to be quite effective in mediating T cell cytotoxicity (Holliger *et al.*, 1996; Kipriyanov *et al.*, 1998; Zhu *et al.*, 1996). However, the co-secretion of two hybrid scFv fragments can give rise to two types of dimer: active heterodimers and inactive homodimers. A second problem is that the two chains of diabodies are held together by non-covalent associations of the V_H and V_L domains and can diffuse away from one another. Moreover, to ensure the assembly of a functional diabody, both hybrid scFv fragments must be expressed in the same cell in similar amounts. This latter requirement is difficult to uphold in eukaryotic expression systems such as yeast, which are often preferred because high yields of enriched product can be obtained (Ridder *et al.*, 1995; Shusta *et al.*, 1998). Finally, the small size of bispecific diabodies (50–60 kDa) leads to their rapid clearance from the blood stream through the kidneys, thus requiring the application of relatively high doses for therapy.

To circumvent the drawbacks of diabodies and to increase the valency, stability and therapeutic potential of recombinant bispecific antibodies, we have now constructed single chain molecules comprising four antibody variable domains (V_H and V_L) of two different specificities in an orientation preventing Fv formation. They can either form bivalent bispecific antibodies by diabody-like folding (sc-diabodies) or dimerize with the formation of tetravalent bispecific antibodies (tandem diabodies). The efficacy of tandem diabody (Tandab) formation is dependent on the length of the linker between two halves of the molecule. Here we show that Tandabs are bispecific and have higher avidity resulting from the bivalency for each specificity. CD3 \times CD19 Tandabs were more potent than the diabody for inducing human T cell proliferation in the presence of irradiated CD19⁺ B cells. In cytotoxic assays, Tandabs were able to retarget human T lymphocytes to malignant B cells. The efficiency of Tandab-mediated cell lysis

also compared favorably to that obtained with a diabody of the same dual specificity. *In vivo* studies demonstrated that tetravalent Tandabs were more stable and were retained longer in the blood of normal mice compared to scFv and diabodies. This bispecific antibody format could therefore prove to be particularly advantageous for cancer immunotherapy.

Results

Design of single chain molecules comprising four antibody variable domains

The concept of dimerizing scFv fragments having a short peptide linker between the two domains to create two antigen-binding sites pointing in opposite directions (Holliger *et al.*, 1993) was extended to single chain molecules containing four antibody variable domains. We previously constructed a CD3 \times CD19 bispecific diabody comprising two hybrid scFv fragments: an anti-human CD3 V_H domain joined to an anti-human CD19 V_L domain by a short linker peptide and an anti-CD19 V_H connected to an anti-CD3 V_L by a similar linker (Kipriyanov *et al.*, 1998). We have now fused these hybrid scFvs into a single chain polypeptide using either a long (20 amino acid residues) (Gly₄-Ser)₄ or short (five amino acid residues) Gly-Gly-Pro-Gly-Ser linker (Figure 1(a)). The short linker design was based on our experience with the generation of stable mono- and bispecific diabodies using a linker mainly derived from the N-terminal part of a murine C_H1 domain that contained a proline residue (Arndt *et al.*, 1999; Kipriyanov *et al.*, 1998; Le Gall *et al.*, 1999). We therefore modified the traditional Gly₄-Ser motif (Holliger *et al.*, 1993; Huston *et al.*, 1988) to include a proline residue. However, the actual linker length is larger because we originally cloned the antibody V_K domains using an anti-sense primer complementary to the 5'-region of the C_K domain gene (Kipriyanov *et al.*, 1996a). Therefore, seven additional amino acid residues introduced by this primer are part of the long (LL) and short (SL) linkers (27 and 12 residues, respectively; Figure 1(a)). The long linker was designed to span the distance between the carboxy terminus of the first pair of V-domains and the amino terminus of the second pair to form a sc-diabody (Figure 1(b)). In contrast, the short linker should prevent intramolecular V_H - V_L pairing and force the four domains to interact with complementary ones of another molecule with the formation of an eight-domain Tandab (Figure 1(c)). It should not be too short, however, since the antigen-binding sites in the middle of the molecule might then be sterically hindered. We therefore chose a 12 residue linker to satisfy these two criteria.

Bacterial expression and purification

The four-domain single chain molecules were expressed as soluble secreted proteins in *Escherichia*

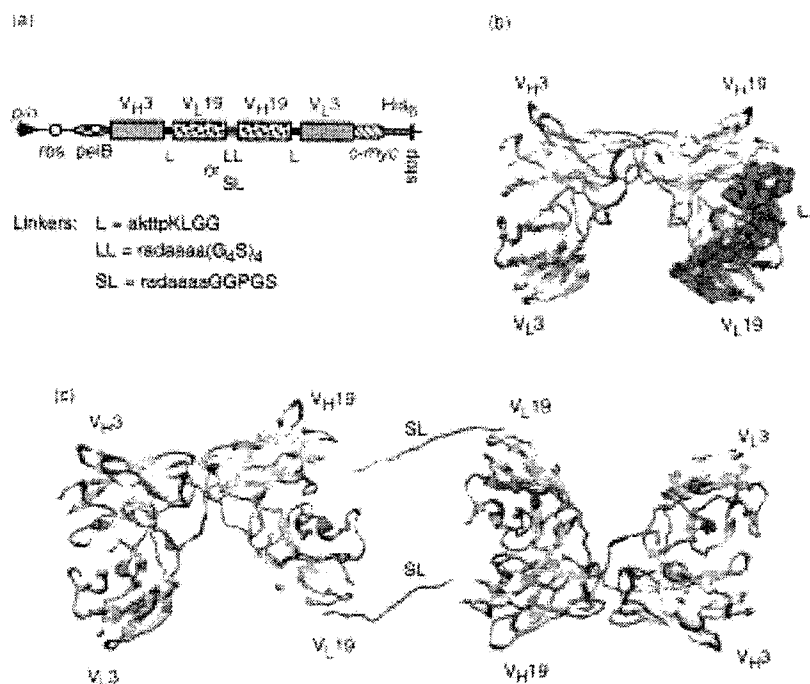


Figure 1. (a) Schematic representation of operons and structural models of (b) sc-diabody and (c) tandem diabody. The locations of promoter/operator (*p/o*), ribosome-binding site (*rbs*), *pelB* leader (*pelB*), *c-myc* epitope (*c-myc*), hexahistidine tag (*his₆*) and stop codon (*stop*) are indicated. The atoms of the long flexible linker (LL) are represented as filled spheres. Beta-sheets are shown in yellow, beta-turns in blue and irregular peptide sequences in green. The positions of anti-CD3 and anti-CD19 variable domains are indicated.

coli. They were isolated from crude periplasmic fractions by immobilized metal affinity chromatography (IMAC). In contrast to IMAC-purified preparations of well-expressed bispecific CD3 \times CD19 diabody (Kipriyanov *et al.*, 1998), those of the four-domain single chain molecules contained large amounts of impurities (Figure 2(a), lane 1). Fortunately, we found that by exchanging the buffer after IMAC for 50 mM imidazole-HCl (pH 6.4-6.7), most of the contaminating bacterial proteins precipitated while the recombinant antibody fragments remained soluble (Figure 2(a), lane 2). In a final step using the cation-exchange chromatography, recombinant single chain molecules were obtained with a purity greater than 95% (Figure 2(b)). On SDS-PAGE, single bands were observed with mobilities quite close to those expected (calculated M_r = 57.1 and 56.2 kDa for single chain molecules with LL and SL, respectively). The corresponding CD3 \times CD19 diabody migrated as two closely spaced protein bands with M_r ~30 kDa (Figure 2(b), lane 1).

Effect of different expression methods on the formation of tandem diabodies

An analysis of the dimerization behavior of four domain single chain molecules was performed by size-exclusion FPLC on a Superdex 200 column in

PBSI buffer (PBS with 50 mM imidazole (pH 7.0)). This buffer was used because, in our experience, PBS alone appeared to be unfavorable for the stability of some antibody fragments, regardless as to whether they had been isolated from inclusion bodies or from soluble periplasmic extracts. For example, buffer exchange for PBS resulted in the aggregation of anti-CD19 scFv and, to a lower extent, of the bispecific CD3 \times CD19 diabody (Kipriyanov *et al.*, 1998). Hydrophobic amino acids from either the V_H/V_L or variable/constant domain interfaces, which are normally buried in the Fab fragment but become exposed to solvent in recombinant scFv (Nieba *et al.*, 1997), might be the cause of aggregation. The use of Tris-HCl or Hepes buffers with high salt concentrations (e.g. 1 M NaCl) can help to solve this problem. Alternatively, the presence of imidazole can stabilize scFv fragments and diabodies (our observation) as well as scFv-RNase fusion proteins (Dr Dianne Newton, personal communication). Empirically, we have determined that PBS with 50 mM imidazole (pH 7.0-7.5), is a suitable buffer for various antibody fragments kept at relatively high concentrations (2-3 mg/ml). Moreover, this buffer did not interfere with antigen binding and did not show any toxic effects after incubation with cultured cells or after injection into mice (intravenous injection of 200 μ l).

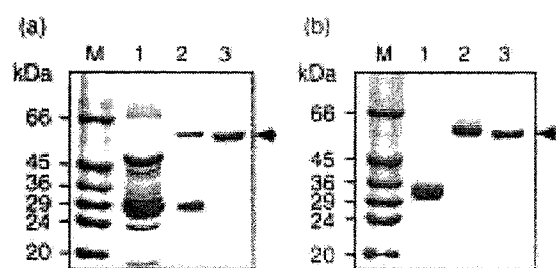


Figure 2. Analyses of bispecific antibody fragments by 12% SDS gel electrophoresis under reducing conditions. (a) SDS-PAGE of the purification of SL-product. Lanes: M, MW markers; 1, sample from IMAC; 2, sample after buffer exchange for 50 mM imidazole-HCl (pH 6.4) and centrifugation; 3, sample eluted from Mono S column. (b) SDS-PAGE of purified bispecific antibody fragments. Lanes: M, markers; 1, diabody; 2, LL product; 3, SL product. The gels were stained with Coomassie brilliant blue. The positions of four domain single chain molecules are indicated.

Size-exclusion chromatography of the LL product purified from bacteria induced in the presence of 0.4 M sucrose (Kipriyanov *et al.*, 1997a) revealed the presence of the monomeric sc-diabody ($M_r \sim 55$ kDa) as well as the homodimer (Tandab) with an apparent $M_r \sim 115$ kDa (Figure 3(b)). We therefore investigated whether the amount of Tandab may depend on the folding history of the protein, and thus on the expression method. The LL and SL products were isolated from periplasmic extracts of *E. coli* cells induced either in normal rich medium or under osmotic stress in the presence of non-metabolized additives such as sucrose (Kipriyanov *et al.*, 1997a) or sorbitol and glycine betaine (Blackwell & Horgan, 1991). As shown in Figure 3, significant increases of the dimeric fractions were obtained using bacteria grown in modified media. As expected, the amount of homodimers was dependent on the linker length. While the LL product comprised almost no dimers using normal medium and about 50% dimers using sorbitol/betaine medium, 80-100% of the SL product was in a dimeric form (Figure 3). In contrast, isolation from inclusion bodies and refolding *in vitro* led exclusively to monomeric LL molecules and predominantly monomeric SL molecules with only 20-30% dimer formation (data not shown). Rechromatography of the first and second peak fractions for both the LL and SL products isolated either from soluble periplasmic extracts or from inclusion bodies yielded only a single species, Tandab or sc-diabody, respectively (data not shown).

The yields of four-domain single chain molecules with LL and SL after expression in *E. coli* shake flask cultures in sorbitol/betaine medium and purification were $0.48(\pm 0.14)$ mg/l per $A_{600 \text{ nm}}$ ($n = 5$) and $0.60(\pm 0.11)$ mg/l per $A_{600 \text{ nm}}$ ($n = 4$), respectively. These values were three- to fourfold

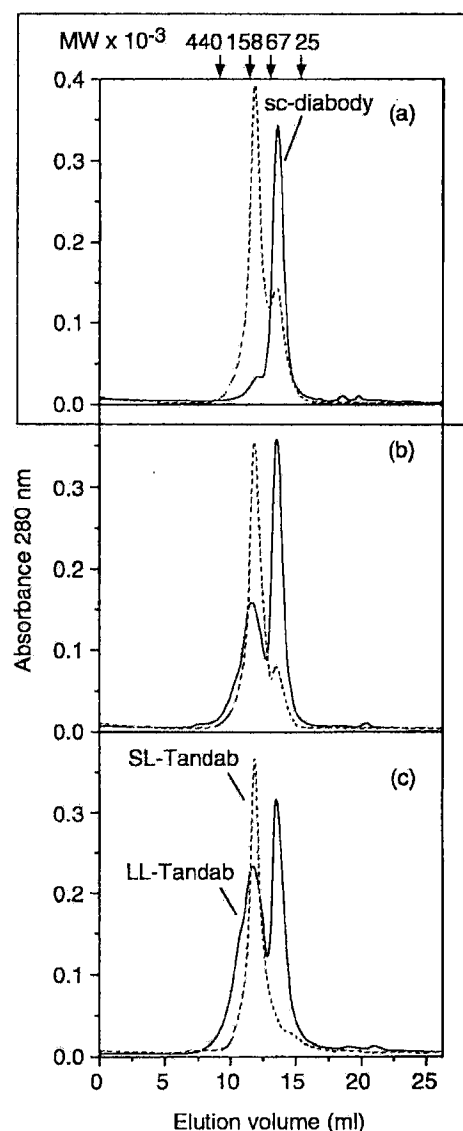


Figure 3. Elution profiles of purified LL product (continuous lines) and SL product (dotted lines) from calibrated Superdex 200 gel filtration column. Antibody fragments isolated from bacteria induced in (a) normal $2 \times \text{YT}$ medium, (b) medium with sucrose and (c) medium with sorbitol and betaine were analyzed. The peaks taken for further *in vitro* and *in vivo* analyses are indicated.

higher than those obtained for material isolated both from inclusion bodies and the soluble periplasmic fraction after expression in normal medium (data not shown). For further analyses, homogeneous preparations of the sc-diabody with the long linker and Tandabs with both the long and short linkers were obtained by isolating the respective peaks after size-exclusion chromatog-

Antigen binding activity

Flow cytometry experiments demonstrated specific interactions with both human CD19⁺ JOK-1 and CD3⁺ Jurkat cells for all the recombinant bispecific antibodies (Figure 4). On a weight basis, the diabody showed the highest fluorescence intensities when interacting with JOK-1 cells and Tandabs gave the highest signals for binding to Jurkat cells. Surprisingly, the sc-diabodies showed higher fluorescence intensities for binding to Jurkat cells, even though they contained only one *c-myc* epitope for immunodetection in contrast to the two peptide tags of the diabodies (Kipriyanov *et al.*, 1998) (Figure 4(b) and (d)).

The CD19 and CD3 binding affinities were estimated by competitive binding to human JOK-1 and Jurkat cells in the presence of either FITC-labeled anti-CD19 MAb HD37 (Pezzutto *et al.*, 1987) or anti-CD3 MAb OKT3 (Kung *et al.*, 1979) (Figure 5(a) and (b)). The relative affinities were calculated from the corresponding IC_{50} values. Compared to the diabody, the sc-diabody bound

CD19 with an almost identical affinity, while the SL and LL-Tandab had affinities that were approximately 1.5 and threefold higher, respectively. Even higher increases in affinity were found for binding to CD3⁺ cells. The sc-diabody, SL and LL-Tandab, respectively, bound CD3 1.5, three- and eightfold more efficiently than the diabody (Table 1).

To investigate the biological relevance of the differences in affinity values of the bispecific molecules, their *in vitro* retention on the surface of both CD3 and CD19-positive cells at 37°C was determined by flow cytometry (Figure 5(c) and (d)). The sc-diabody had a relatively short retention half-life ($t_{1/2}$) on CD19⁺ JOK-1 cells, almost identical with the $t_{1/2}$ of the diabody (Table 1). In contrast, both the tandem diabodies were retained significantly longer on the surface of JOK-1 cells (Table 1). The half-lives of all the bispecific antibodies on the surface of CD3⁺ Jurkat cells were relatively short (Figure 5(d) and Table 1), reflecting the lower CD3 binding affinities deduced from inhibition experiments (Figure 5(b)). In contrast to the diabody and sc-diabody, both tandem diabo-

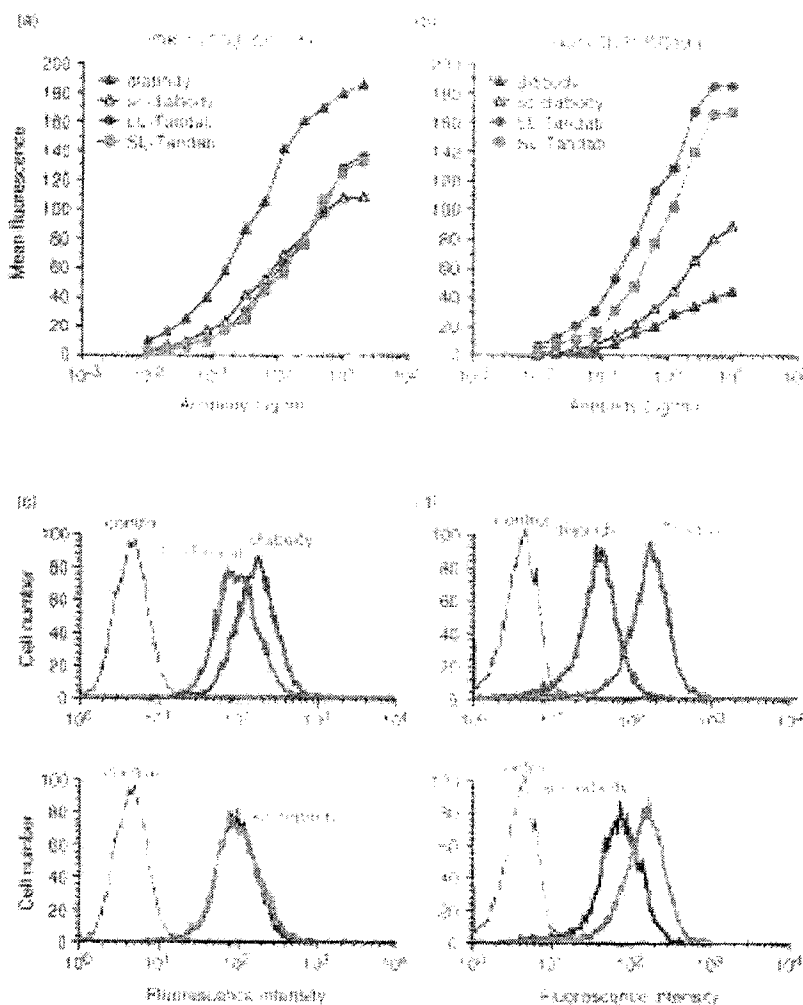


Figure 4. Flow cytometric analysis of antibody fragments binding to (a), (c) CD19⁺/CD3⁻ JOK-1 cells and (b), (d) CD3⁺/CD19⁻ Jurkat cells. (a) and (b) Fluorescence dependence on antibody concentration. (c) and (d) Overlay plots obtained for antibodies at 10 µg/ml concentration.

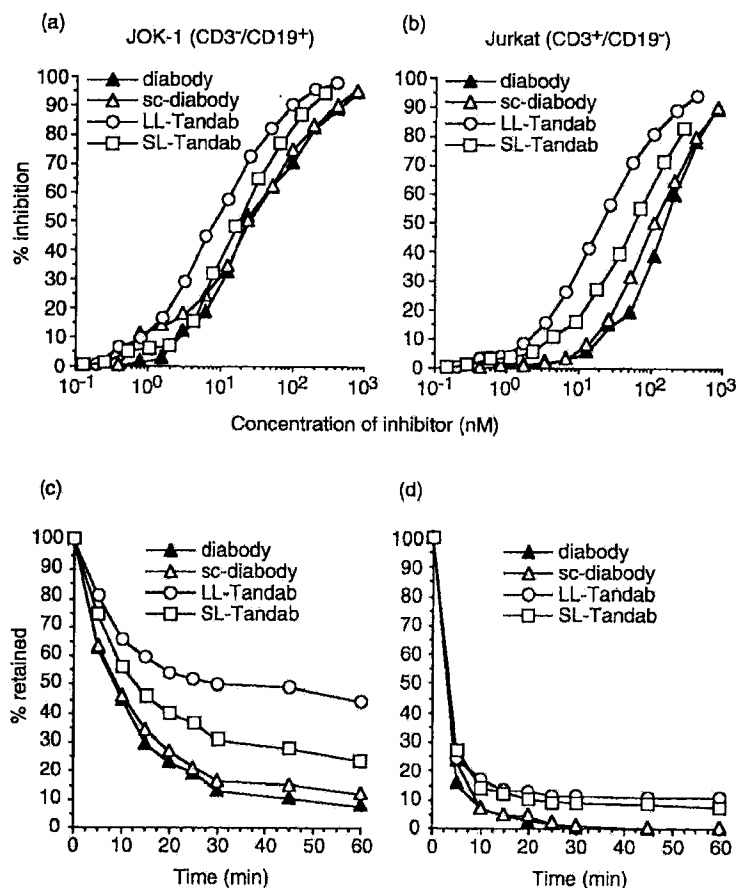


Figure 5. Analyses of apparent affinities by (a), (b) flow cytometry and (c), (d) by cell surface retention *in vitro*. Inhibition of binding of (a) FITC-labeled MAb HD37 to JOK-1 cells and (b) FITC-labeled MAb OKT3 to Jurkat cells in the presence of bispecific antibody fragments are shown. Analogously, cell surface retention profiles were determined either with JOK-1 or (d) Jurkat cells.

dies demonstrated a biphasic decay of fluorescence intensity associated with Jurkat cells (Figure 5(d)). The fast half-life ($t_{1/2\alpha}$) of both Tandabs was nearly identical with the $t_{1/2}$ of the sc-diabody, while the slow half-life ($t_{1/2\beta}$) was almost threefold longer than $t_{1/2\alpha}$ (Table 1). This biphasic dissociation of the Tandabs may indicate the presence of subpopulations of Jurkat cells with different densities of the CD3 ϵ epitope on their surface.

Biological activity

Two *in vitro* tests were used for comparing the biological activity of the bispecific antibodies. First, their ability to stimulate T cell proliferation when bound to the surface of tumor cells was determined. Irradiated CD19⁺ Raji cells were treated with different concentrations of each bispecific antibody and subsequently incubated in the presence of human PBL prestimulated with a low-dose of IL-2. As shown in Figure 6(a), diabody treatment resulted in a strong dose-dependent increase in T cell proliferation. In comparison, the SL-Tandab performed significantly better and the LL-Tandab showed the highest stimulatory effect.

The second test measured the ability of the bispecific molecules to induce tumor cell lysis by

redirecting T cell cytotoxicity. At a concentration of 10 μ g/ml, the sc-diabody was as potent as the diabody in mediating tumor cell killing by activated human PBL but was slightly less potent than both of the Tandabs (Figure 6(b)). Comparisons of cell apoptosis efficiency at various molar concentrations of the bispecific antibodies demonstrated a consistently better performance of the Tandabs (Figure 6(c) and (d)).

Stability *in vitro*

One of the most important applications of BsAbs is in cancer therapy where factors such as plasma half-life and tumor penetration play an important role. The BsAb should also be stable at 37°C in human serum to have a significant anti-tumor effect. We therefore analyzed the antigen-binding activity of the recombinant BsAb molecules when stored at a fairly low concentration in human serum at 37°C for prolonged periods of time. A concentration of 15 μ g/ml was chosen in order to avoid the fluorescence plateau in FACScan analysis (Figure 4). The residual activity was estimated by flow cytometry with CD3⁺ Jurkat cells, since the CD3-binding activity of the diabody was previously shown to be less stable than the CD19-

Table 1. Affinity and binding kinetics of recombinant bispecific molecules

Antibody	Valency ^a	IC ₅₀ ^b (nM)	K _D ^b (nM)	k _{off} fast ^c (s ⁻¹ /10 ⁻³)	t _{1/2} α ^c (minutes)	k _{off} slow ^c (s ⁻¹ /10 ⁻³)	t _{1/2} β ^c (minutes)
A. JOK-1 cells (CD3⁻/CD19⁺)							
Diabody	M	25.25	1.29	1.16 ± 0.28	10.0	N.D.	N.D.
sc-diabody	M	26.61	1.36	1.05 ± 0.30	11.0	N.D.	N.D.
LL-Tandab	B	9.19	0.47	0.48 ± 0.18	24.3	N.D.	N.D.
SL-Tandab	B	20.45	1.05	0.74 ± 0.22	15.7	N.D.	N.D.
B. Jurkat cells (CD3⁺/CD19⁻)							
Diabody	M	154.58	15.46	3.97 ± 1.42	2.9	N.D.	N.D.
sc-diabody	M	108.18	10.82	3.44 ± 1.02	3.4	N.D.	N.D.
LL-Tandab	B	20.04	2.00	3.30 ± 1.27	3.5	1.04 ± 0.50	11.2
SL-Tandab	B	57.80	5.78	3.31 ± 0.99	3.5	1.17 ± 0.53	9.8

N.D., not determined.

^a Putative valency for each specificity. M, monovalent; B, bivalent.^b Deduced from inhibition experiments.^c Deduced from cell surface retention assays.

binding activity (Kipriyanov *et al.*, 1998). We found that all of the bispecific molecules retained 80-90% of their antigen binding activity after 24 hours incubation at 37°C in human serum (Figure 7(a)). Prolonged incubation demonstrated that single chain molecules appeared to be more stable than the non-covalent dimer diabody with 1.5 to 2.5-

fold increased half-lives (Table 2). For example, even after incubation for one week at 37°C, the LL-Tandab retained 40% of its activity (data not shown). Western blot analyses of the samples of bispecific molecules showed no proteolytic degradation for any of them after 81 hours of incubation in human serum at 37°C (data not shown).

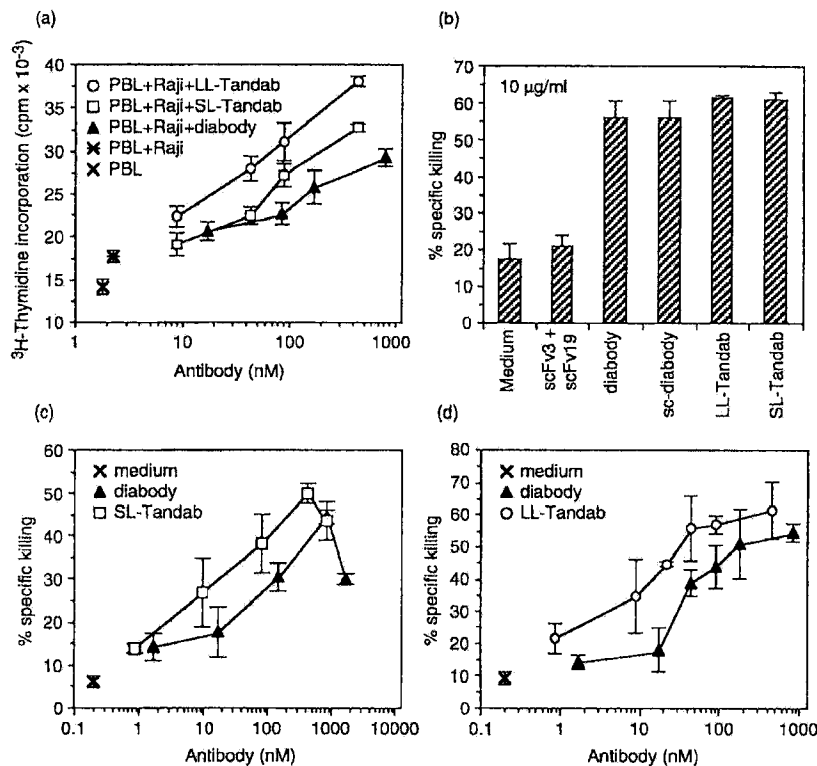


Figure 6. Biological activity of diabodies and tandem diabodies. (a) BsAb stimulation of activated human T cell proliferation in the presence of irradiated CD19⁺ Raji cells. (b)-(d) BsAb mediated killing of Raji cells by activated human PBL as determined by a JAM test. Effector:tumor cell ratio was 25:1. (b) Antibody fragments were used at concentration of 10 µg/ml. Mean values ± SE are plotted.

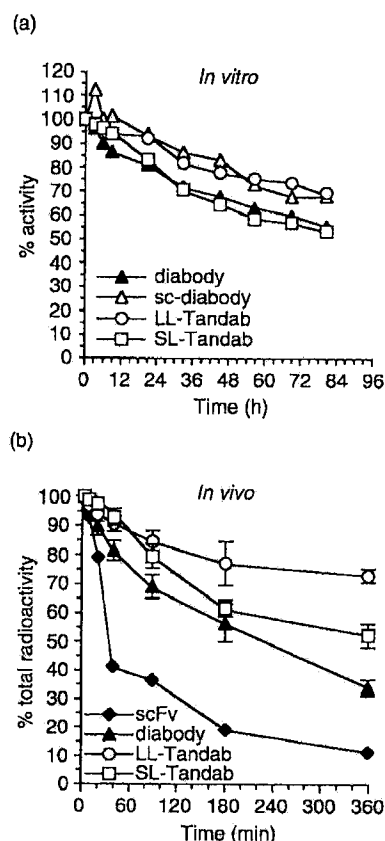


Figure 7. *In vitro* and *in vivo* stability of bispecific antibody fragments. (a) Stability in human serum at 37°C as determined by flow cytometry using CD3⁺ Jurkat cells. Activities of the samples at point zero were taken as 100%. (b) *In vivo* stability of ¹²⁵I-labeled antibody fragments. Protein-bound radioactivity in TCA precipitated plasma samples were calculated as percentages of the total radioactivity (TCA-pellet and supernatant) at specific time points. The values up to six hours after administration of the labeled compounds are plotted as mean values \pm SE.

Blood clearance and stability *in vivo*

To compare the plasma clearance pharmacokinetics of Tandabs and smaller antibody fragments, we administered preparations of ¹²⁵I-labeled anti-human CD3 scFv monomer (30 kDa) (Kipriyanov *et al.*, 1997b), CD3 \times CD19 diabody (58 kDa) (Kipriyanov *et al.*, 1998), LL-Tandab (114 kDa) and SL-Tandab (113 kDa) intravenously to mice. Blood samples were taken at various time points. To exclude errors in calculating plasma half-lives due to free radioiodine resulting from cellular, metabolic degradation of labeled protein, we first determined the proportion of protein-bound radioactivity for each plasma sample by TCA precipitation. As can be seen in Figure 7(b), TCA-precipitable radioactivities of scFv decreased rapidly in the blood over time, only 50% of the radioactivity were bound to protein 30 minutes after the

intravenous injection. In contrast, the diabody lost its label much more slowly, more than 50% of its radioactivity could be precipitated three hours after injection. The Tandabs were even more stable: 72 and 52% of the radioactivity was found to be associated with protein six hours after administration of the LL and SL-Tandab, respectively (Figure 7(b)). The estimated half-lives of the diabody and the Tandabs exceeded that of the scFv three- and sixfold, respectively (Table 2). SDS-PAGE analysis followed by autoradiography showed no degradation of either Tandab 1.5 hours after injection (data not shown).

Analyses of blood samples at different time points demonstrated an extremely rapid clearance of scFv from plasma, with an alpha-phase (extravasation and renal clearance) half-life ($t_{1/2\alpha}$) of 3.5 minutes and a beta-phase (catabolism) ($t_{1/2\beta}$) of 74.6 minutes (Figure 8). The diabody had an approximately twofold slower first-pass clearance and a somewhat slower catabolism (Figure 8 and Table 2). Even slower plasma clearance rates were observed for the larger Tandabs (Figure 8). Alpha-phase half-lives were estimated to be four- and eightfold higher for the SL and LL-Tandabs, respectively, in comparison to that of scFv (Table 2). The pharmacokinetic areas under the curves (AUC) were calculated for all of the antibody fragments to provide a means of estimating the total relative dose that would be delivered in a therapeutic application. Tandem diabodies demonstrated the best pharmacokinetic performance, their AUC values were two- and fivefold higher than AUC values calculated for the diabody and scFv, respectively (Table 2). The differences in the pharmacokinetic properties of these constructs correlate quite well with their size.

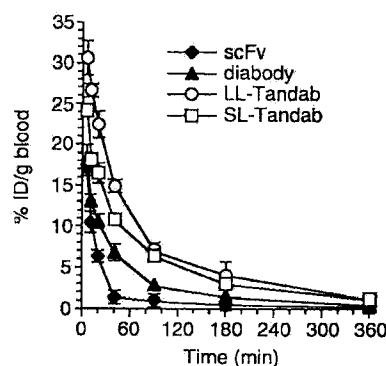


Figure 8. Pharmacokinetics of plasma retention of ¹²⁵I-labeled antibody fragments in mice. Blood samples were obtained at the times indicated. Data were corrected for non-TCA-precipitable radioactivity. The values up to six hours after administration of the labeled compounds are plotted as mean values \pm SE.

Table 2. *In vitro* and *in vivo* stability and pharmacokinetic parameters for scFv and bispecific antibody fragments

Antibody fragment	Stability ^a		Blood clearance $t_{1/2\alpha}$ (minutes)	Pharmacokinetics ^b	
	<i>in Vitro</i> $t_{1/2}$ (hours)	<i>in Vivo</i> $t_{1/2}$ (hours)		$t_{1/2\beta}$ (minutes)	AUC %ID/g per minute
scFv	N.D.	1.2	3.5	74.6	422.4
Diabody	63.0	3.1	8.4	91.9	1123
sc-diabody	157.7	N.D.	N.D.	N.D.	N.D.
LL-Tandab	126.2	7.3	28.5	119.7	2919
SL-Tandab	87.3	6.8	11.9	92.5	2234

N.D., not determined.

^a The half-life values for stability measurements were deduced from the one phase exponential decay fit of experimental data presented in Figure 7 and were calculated as $\ln 2/k$.

^b To estimate the blood retention half-lives, a bi-exponential function was fitted to each blood clearance curve (Figure 8) after correcting for metabolic degradation of labeled protein. The therapeutic effectiveness of the analyzed antibody fragments was also compared by integration of the blood retention curves. The areas under the curve (AUC) were measured to infinite time with each curve being represented as a bi-exponential function.

Discussion

We have constructed novel recombinant bispecific tetravalent antibody fragments that we have named "tandem diabodies", since their design is based on the intermolecular pairing of V_H and V_L domains as described for diabodies (Holliger *et al.*, 1993). Although the non-covalent forces holding the V_H and V_L domains together are fairly weak, often resulting in Fv dissociation (Glockshuber *et al.*, 1990), the association of two V_H/V_L pairs in a dimer of V_H-V_L fusion proteins (diabody) provides a relatively stable structure (Holliger *et al.*, 1993; Kipriyanov *et al.*, 1998). This observation prompted us to consider whether single chain molecules consisting of four variable domains of two different specificities would form a stable homodimer with four antigen-binding sites. In contrast to previously described bivalent and bispecific scFv-scFv tandems (Gruber *et al.*, 1994; Kurucz *et al.*, 1995), this new class of tandem diabodies are tetravalent. The results presented here demonstrate that such Tandabs can be obtained in a functional form from *E. coli* by fusing two hybrid variable domain pairs in a single polypeptide. The order of V-domains and the linker peptides between them were designed such that each domain pairs with a complementary domain in another molecule (Tandab) or in the other half of the same molecule (single chain diabody).

Since our antibody fragments have genetically fused hexahistidine tags, we used immobilized metal affinity chromatography for the isolation of recombinant products from crude bacterial periplasmic extracts. If the His-tagged protein is highly over-expressed in *E. coli*, a one-step IMAC purification can result in sufficiently pure material for most applications (Casey *et al.*, 1995; Kipriyanov *et al.*, 1998). However, if the protein of interest is present only as a small fraction, several contaminating bacterial proteins can bind to the IMAC column under the purification conditions and co-elute (for a list of histidine-rich *E. coli* proteins, see Müller *et al.*, 1998a). For further purification of antibody fragments from IMAC-eluted material,

either antigen-affinity chromatography (Kipriyanov *et al.*, 1994), thiophilic adsorption chromatography (Müller *et al.*, 1998b; Schulze *et al.*, 1994) or immunoaffinity purification using immobilized anti-His-tag monoclonal antibodies (Müller *et al.*, 1998a) have been used. Here, we describe a relatively simple alternative procedure based on the separation of proteins according to their solubility in imidazole-HCl buffer. We found that poorly expressed antibody fragments eluted from IMAC columns can be further enriched by buffer exchange with 50 mM imidazole-HCl (pH 6.4), and subsequently purified to homogeneity by ion-exchange chromatography in the same buffer. This approach was tested for a number of scFv-based recombinant proteins and seems to be generally applicable.

The dimerization of the four-domain single chain molecules proved to be dependent on the expression method. Dimers were probably a product of domain swapping (Bennett *et al.*, 1994) when obtained from soluble periplasmic extracts, whereas predominantly monomers were isolated from inclusion bodies after refolding. Similar observations on the formation of scFv dimers were made by Arndt *et al.* (1998). Major differences between periplasmic folding and refolding *in vitro* include high protein concentrations in the periplasm and the presence of bacterial chaperones. A rough estimation of the concentration of recombinant antibody during folding in the periplasmic space of bacteria indicated a 500-fold difference to the low concentrations employed for folding *in vitro* (Arndt *et al.*, 1998). The domain-swapped dimer is increasingly favored when the concentration of the protein increases (Schlunegger *et al.*, 1997). Some other unknown factors in the periplasm might also influence dimerization. Here, we demonstrate for the first time that inducing synthesis of recombinant antibody fragments in bacteria under osmotic stress promotes the formation of domain-swapped dimers. We tested the effect of adding non-metabolized low molecular mass compounds to the normal growth medium. These were 0.4 M sucrose and 1 M sorbitol in combination with 2.5 mM gly-

cine betaine, both of which were previously shown to inhibit aggregation and encourage correct folding of recombinant proteins in *E. coli* (Blackwell & Horgan, 1991; Bowden & Georgiou, 1990; Kipriyanov *et al.*, 1997a; Sawyer *et al.*, 1994). Although little is known about the mechanism of action of sucrose, sorbitol, or betaine on protein folding *in vivo*, these compounds appear to stabilize protein structures *in vitro* (Arakawa & Timasheff, 1985; Lee & Timasheff, 1981; Xie & Timasheff, 1997).

Dimers of the four-domain single chain molecules probably take the form of domain-swapped tandem diabody (Figure 1(c)). It is very likely that a high-energy barrier must be overcome for sc-diabody to open up and dimerize, as illustrated in Figure 9. To pass from a closed monomer (Figure 9(a)) to a domain-swapped dimer

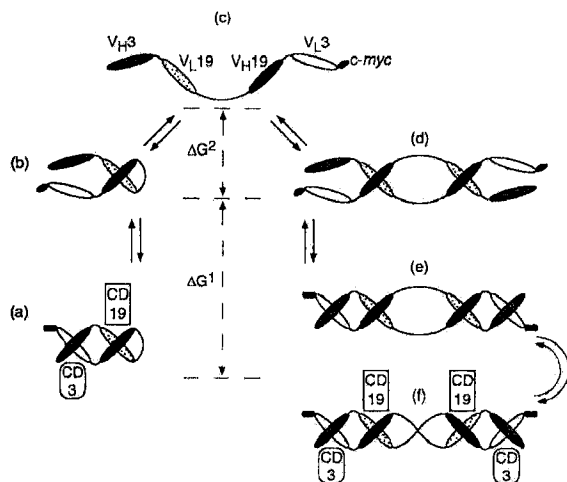


Figure 9. Model of putative pathways leading to sc-diabodies and domain-swapped dimers. The model describes the monomeric and dimeric species in three different forms, an open, a double open and a closed form. (a), (f) The closed form represents the stable bispecific molecule with intact V_H/V_L interfaces that is able to bind both antigens and cross-link two cells. (b), (d) In the open form, only half of the V_H/V_L complexes are formed, the two complementary domains can separate but are not able to change the oligomerization state. (c) The double open form represents the conformation of a monomer with no paired V-domains, which can adopt either the mono- or dimeric conformation. The V_H and V_L domains of both specificities as well as the C-terminal *c-myc* epitope are indicated. The filled arrows indicate possible transition pathways. The broken arrows illustrate putative free energy relationships between different monomeric and dimeric forms and indicate the presence of two transition steps. Depending on experimental conditions, either the monomer or the dimer can be the more stable molecular form. Tandabs shown in (e) and (f) illustrate different conformational states of the closed dimer. It is quite probable that after the first binding event to a cell surface the conformation of the dimer adjusts to enable bivalent binding to the same cell and the cross-linking of two cells.

(Figure 9(f)), the sc-diabody must first pass through the open monomer form in which non-covalent bonds of the V_H/V_L interface are broken (Figure 9(b)). The sc-diabody is a functional four-domain protein stabilized by the non-covalent association of two V_H/V_L pairs (Figure 9(a)). These interactions can be substantial since the dissociation constants for Fv fragments can be in the range of 1-100 nM (Givol, 1991; Mallender *et al.*, 1996; Polymenis & Stollar, 1995). The energy barrier would probably be much higher than that required for the formation of Fv dimers (Arndt *et al.*, 1998), since a double open monomer is needed for swapping each domain (Figure 9(c)). The latter requirement can probably only be achieved under denaturing conditions. The same forces that stabilize the association of domains in the monomer must stabilize the dimer. Accordingly, the transition from a closed Tandab (Figure 9(e) and (f)) to the double open monomer (Figure 9(c)) requires the consecutive dissociation of four V_H/V_L complexes. This could explain why we did not see any interconversion between the sc-diabody and the Tandab *in vitro*, for example, under conditions of constitutive dilution during the re-chromatography of Tandabs, as was previously observed for non-covalent scFv dimers (Kipriyanov *et al.*, 1994), or during the concentration of the sc-diabody (data not shown). The incubation of Tandabs at 37°C for prolonged periods of time also did not cause any large decreases in antigen binding as would be expected for a dimer-monomer transition (Figures 4 and 7). It is therefore quite probable that the four-domain single chain molecules undergo dimerization during folding *in vivo*. This would occur if the association of folded domains is slow relative to domain folding. When closed monomer-stabilizing conditions are provided, the open monomers (Figure 9(c)) may either fold "head-to-tail" (Figure 9(b)) or swap domains with complementary ones of another molecule (Figure 9(d)). The solvent additives such as sucrose, sorbitol and betaine might affect the rate of intramolecular and intermolecular domain pairing and thus shift the monomer/dimer balance. For example, it was previously shown that the protein structure stabilizing properties of sucrose, sorbitol and betaine reflect their stronger exclusion from the unfolded protein than from the native structure (Arakawa & Timasheff, 1985; Lee & Timasheff, 1981; Xie & Timasheff, 1997). This interaction makes it thermodynamically unfavorable for proteins to unfold. An additional possibility is that the stabilizers influence periplasmic factors involved in protein folding.

We propose that both the diabody and the sc-diabody have fairly similar structures (Figure 1(b)), which appear to be reflected in their very close antigen-binding and biological characteristics. However, the linker of the sc-diabody may give rise to conformational changes in the V_H/V_L interface, since the sc-diabody bound with

somewhat higher affinity to CD3⁺ cells than the diabody (Figure 4 and Table 1). Surprisingly, the diabody showed the highest fluorescence intensities on a weight basis among all examined antibodies when interacting with JOK-1 cells (Figure 4(a) and (c)). However, competition binding assays and cell-surface retention experiments demonstrated that the enhanced fluorescence signals of the diabody were not caused by enhanced affinity (Table 1); they are probably due to the smaller size of the diabody thus facilitating its binding to less accessible cell-anchored CD19 antigens or better presentation of the two *c-myc* epitopes for immunodetection.

Compared with the CD3 × CD19 diabody, the Tandabs exhibited a higher apparent affinity of antigen binding and slower dissociation from both CD3⁺ and CD19⁺ cells. *A priori*, it was unclear to what extent an affinity increase would occur with a Tandab that is potentially bivalent for each antigen. For example, the distance between the antigen-binding sites of the same specificity was expected to be shorter in the Tandab than in the IgG molecule. Furthermore, unlike the flexible Fab arms of an IgG that freely rotate on the hinge, the Tandab seemed to have a fairly rigid configuration (Figure 1(c)). If antigen-binding sites of the same specificity occurred only on different sides of the diabody tandem, bivalent cell binding would not have been possible. However, the cell surface retention assay clearly demonstrated bivalent cell binding for both of the Tandabs. A closer examination of the SL-Tandab model from a different perspective (top view) showed a boomerang-shaped symmetric structure with the two halves oriented at an angle of about 165° and separated by the two crossed linkers (Figure 10). The CDR loops of both CD19-binding sites appear to project in one direction, just opposite to the orientation of the anti-CD3 parts of the molecule. The distances

between the CD19-binding sites in the SL and LL-Tandabs were estimated to be 55 and 110 Å, respectively. Moreover, the CD3-binding sites, even in the SL-Tandab, can span a distance of up to 150 Å, which is similar to the stretch of Fab arms in an IgG molecule (Harris *et al.*, 1998). The molecular model was thus consistent with our experimental findings.

The length of the linker appeared to have some influence on antigen binding, since the LL-Tandab showed a significantly lower K_D and slower k_{off} from CD19-positive cells than the SL-Tandab (Table 1). This could be due to the larger distance between CD19-binding sites in the LL molecule and/or the higher flexibility and freedom of rotation that facilitate bivalent interaction with the cell. In contrast to their dissociation from CD19⁺ cells, we did not observe any difference in k_{off} between LL and SL-Tandabs for dissociation from CD3⁺ cells (Figure 4 and Table 1). This may indicate that the distance between the CD3-binding sites is sufficient in both molecules to achieve bivalent binding. In addition, the linker may affect the globular structure of Tandabs, which could account for the observed differences in their pharmacokinetic parameters.

The Tandabs were consistently more effective than the diabody for inducing T cell proliferation in the presence of tumor cells and in effector cell retargeting. As expected, both Tandabs had lower clearance rates compared to smaller antibody fragments such as the scFv and the diabody. The pharmacokinetic parameters ($t_{1/2}$ and AUC) of Tandabs proved to be quite similar to those of 100 kDa F(ab')₂ fragments and exceeded those of the smaller (scFv')₂ and Fab fragments (for a review, see Adams, 1998). We have shown here that both the sc-diabody and the Tandab are significantly more stable than the diabody *in vitro* and *in vivo* (Figure 7 and Table 2). They might therefore be

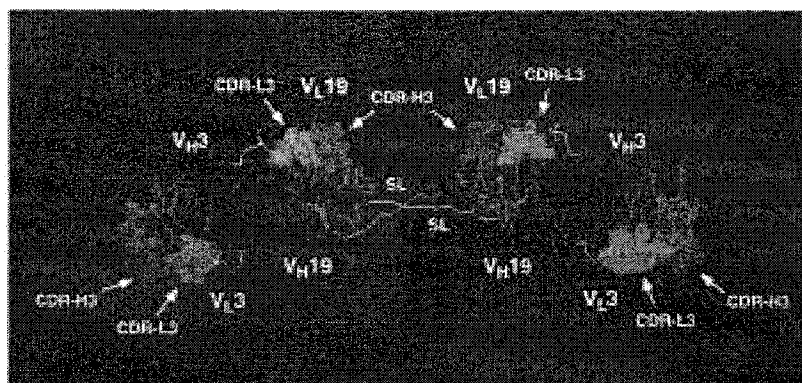


Figure 10. Structural model of SL-Tandab (top view). Anti-CD3 V_H and V_L domains are shown in red and green, anti-CD19 V_H and V_L in magenta and cyan, respectively. The linkers between V-domains and the SL-linkers are shown in yellow and white, respectively. To indicate the antigen-binding sites, the residues of the most hypervariable CDR-3 loops of either V-domain are shown in a spacefill mode. The Figure was generated using a molecular visualization program RasMol v2.5 (Roger Sayle, Biomolecular Structure, Glaxo Research and Development, Greenford, Middlesex, UK).

more useful than the smaller monovalent or bivalent antibody fragments for clinical applications where longer serum performance times are desirable. A further advantage of Tandabs is that they are homodimers stabilized by four interdomain pairings that assemble from a single homogeneous expression product. The bispecific diabody preparations, on the other hand, usually contain a significant proportion of non-functional homodimers (Zhu *et al.*, 1996, 1997), which makes it difficult to obtain a pure homogeneous product. If the Tandab dissociates, it can still form a functional single chain diabody. The construction of a sc-diabody is an alternative way to stabilize a bivalent bispecific diabody in addition to the incorporation of an intermolecular disulfide bridge or a knob-into-hole approach (FitzGerald *et al.*, 1997; Zhu *et al.*, 1997).

The novel bispecific recombinant molecules described here are potential immunotherapeutic agents for treating B cell leukemias and malignant lymphomas, since they bind to the human B cell surface antigen CD19 and the CD3 ϵ chain of the human CD3/TCR complex. Two different approaches have been used previously to generate tetravalent bispecific antibodies: scFv fusion to whole IgG (Coloma & Morrison, 1997) and dimerization of scFv-scFv tandems *via* a linker containing a helix-loop-helix motif (Müller *et al.*, 1998b). In contrast, tandem diabodies comprise only antibody variable domains without the need of extra self-associating structures. To reduce the risk of an immune reaction, appropriate V_H and V_L fragments could be selected from a human antibody library. The linkers can also be easily replaced with ones of human origin. Tandem diabodies are therefore an attractive alternative to existing antibody-derived therapeutics for clinical applications.

Materials and Methods

Molecular modeling

A 3D model of the CD3 \times CD19 diabody was generated using the Internet-based homology modeling software (WHATIF) of the EMBL BioComputing unit (<http://swift.embl-heidelberg.de/servers/>) (Rodriguez *et al.*, 1998). The experimentally solved structure of a bivalent diabody (PDB-entry 1LMK) (Perisic *et al.*, 1994) and a model of the OKT3 derived Fv fragment (Kipriyanov *et al.*, 1997b) were used as templates. The model optimization was performed using the Biopolymer option of Insight II (Molecular Simulations, San Diego, CA). A preliminary 3D structure of the 27 residue long linker was constructed by hand using the Protein option of the Insight II. This model was attached to the diabody structure to link the C terminus of V_L19 with the N terminus of V_H19. The linker was allowed to equilibrate and fit smoothly to the surface of the diabody by running molecular dynamic simulations at 300 K for 100 ps. During the simulation, only the atoms of the constructed linker were allowed to move. The model of the tandem diabody was constructed in a similar way with the exception that no molecular dynamic simulations were performed because of the large computational power required for molecules of such a size.

Plasmid construction

For all the cloning steps and DNA isolation, the *E. coli* K12 strain XL1-Blue (Stratagene, La Jolla, CA) was used. Plasmids pHOG3-19 and pHOG19-3 coding for hybrid V_H3-V_L19 and V_H19-V_L3 scFvs (Kipriyanov *et al.*, 1998) were used for assembly of sc-diabody and Tandab genes. The gene encoding scFv3-19 was amplified by PCR with the primers Bi3sk, 5'-CAG CCG GCC ATG GCG CAG GTG CAA CTG CAG CAG and either Li-1, 5'-TAT ATA CTG CAG CTG CAC CTG GCT ACC ACC ACC ACC GGA GCC GCC ACC ACC GCT ACC ACC GCC GCC AGA ACC ACC ACC ACC AGC GGC CGC AGC ATC AGC CCG to generate a long flexible (Gly₄Ser)₄ intramolecular linker (PCR fragment 1) or Li-2, 5'-TAT ATA CTG CAG CTG CAC CTG CGA CCC TGG GCC ACC AGC GGC CGC AGC ATC AGC CCG to generate a short rigid Gly-Gly-Pro-Gly-Ser linker (PCR fragment 2). The expression plasmids pDISC1-LL and pDISC2-SL were constructed by ligation of the *Nco*I/*Pvu*II restriction fragment from pHOG19-3 comprising the vector backbone and the *Nco*I/*Pvu*II digested PCR fragments 1 and 2, respectively.

The improved expression vectors were constructed to include the *hok/sok* plasmid-free cell suicide system (Thisted *et al.*, 1994) and a gene encoding the Skp/OmpH periplasmic factor for higher recombinant antibody production (Bothmann & Plückthun, 1998). The *skp* gene was amplified by PCR with primers *skp*-1, 5'-CGA ATT CTT AAG ATA AGA AGG AGT TTA TTG TGA AAA AGT GGT TAT TAG CTG CAG G and *skp*-2, 5'-CGA ATT AAG CTT CAT TAT TTA ACC TGT TTC AGT ACG TCG G using as a template the plasmid pGAH317 (Holck & Kleppe, 1988) kindly provided by Dr R. Chen (Max-Planck Institute for Biology, Tübingen, Germany). The resulting PCR fragment was digested with *A*fII and *H*indIII and cloned into the *A*fII/*H*indIII linearized plasmid pHKK (Horn *et al.*, 1996) (kind gift of Dr D. Riesenberger, NKI, Jena, Germany) generating the vector pSKK1. The genes coding for four domain single chain molecules in plasmids pDISC1-LL and pDISC2-SL were amplified by PCR with primers *fe*-1, 5'-CGA ATT TCT AGA TAA GAA GGA GAA ATT AAC CAT GAA ATA CC and *fe*-2, 5'-CGA ATT CTT AAG CTA TTA GTG ATG GTG ATG GTG ATG TGA G. The *X*baI/*A*fII digested PCR fragments were cloned into pSKK in front of the *skp* insert resulting in expression plasmids pDISC5-LL and pDISC6-SL containing tri-cistronic operons (*lacZ'*, gene encoding the four domain single chain molecule, *skp*) under the control of the *lac* promoter/operator system.

For expression of four-domain single chain molecules as periplasmic inclusion bodies, the *Eco*RI/*X*baI fragments of plasmids pDISC1-LL and pDISC2-SL comprising antibody genes preceded by a PelB leader sequence were cloned into pOPE51 (Kipriyanov *et al.*, 1994) generating the expression vectors pOPE-LL and pOPE-SL, respectively. The sequences of all newly constructed genes and plasmids were verified by restriction digests and dideoxy sequencing (Sanger *et al.*, 1977).

Protein expression and purification

For functional expression of recombinant antibodies in the bacterial periplasm, the plasmids pDISC5-LL and pDISC6-SL were transformed into *E. coli* K12 strain RV308 (Δ *lacZ*74 *gal*II::OP308*strA*) (Maurer *et al.*, 1980)

kindly provided by Dr A. Plückthun (University of Zürich, Zürich, Switzerland). Transformed bacteria were grown overnight in shake flasks containing $2 \times \text{YT}$ medium with 0.1 g/l ampicillin and 100 mM glucose ($2 \times \text{YT}_{\text{GA}}$) at 26°C. Dilutions (1:50) of the overnight cultures in $2 \times \text{YT}_{\text{GA}}$ were grown as flask cultures at 25°C with shaking at 200 rpm. When cultures reached $A_{600 \text{ nm}} = 0.6$, bacteria either were induced by adding IPTG to a final concentration of 0.2 mM or were harvested by centrifugation at 20°C. The pelleted bacteria were resuspended in the same volume of either fresh $2 \times \text{YT}_{\text{SA}}$ ($2 \times \text{YT}$ containing 0.1 g/l ampicillin and 0.4 M sucrose; Kipriyanov *et al.*, 1997a) or YTBS medium ($2 \times \text{YT}$ containing 1 M sorbitol and 2.5 mM glycine betaine; Blackwell & Horgan, 1991). IPTG was added to a final concentration of 0.2 mM and growth was continued at 24°C for 14–16 hours. The bacterial cells were then harvested by centrifugation and periplasmic extracts were isolated as previously described (Kipriyanov *et al.*, 1997a,b). The periplasmic fractions were dialyzed against start buffer (50 mM Tris-HCl, 1 M NaCl, pH 7.0) at 4°C. The four-domain single chain molecules were purified by IMAC using Ni-NTA-Superflow resin (Qiagen, Hilden, Germany). After washing with start buffer containing 20 mM imidazole (pH 7.0), the absorbed protein was eluted with 0.3 M imidazole in start buffer (pH 7.0). The elution fractions containing recombinant antibodies were identified by Western blot analysis using anti-*c-myc* MAb 9E10 (IC Chemikalien, Ismaning, Germany) performed as previously described (Kipriyanov *et al.*, 1994). Positive Western blot fractions were pooled and subjected to buffer exchange for 50 mM imidazole-HCl (pH 6.4) using pre-packed PD-10 columns (Pharmacia Biotech, Freiburg, Germany). The turbidity of protein solution was removed by centrifugation. The final purification of four domain single chain molecules was achieved by ion-exchange chromatography on a Mono S HR5/5 column (Pharmacia) in 50 mM imidazole-HCl (pH 6.4), with a linear 0–1 M NaCl gradient. The purified antibody preparations were concentrated and resolved by size-exclusion FPLC on a Superdex 200 HR10/30 column (Pharmacia) in PBSI (15 mM sodium phosphate, 0.15 M NaCl, 50 mM imidazole, pH 7.0). Sample volumes for analytical and preparative chromatographies were 50 and 500 μl , respectively. The column was calibrated with high and low molecular mass gel filtration calibration kits (Pharmacia). All purification procedures were performed at 4°C. Isolation of the anti-CD3 scFv and CD3 \times CD19 diabody was performed as described (Kipriyanov *et al.*, 1997b, 1998).

Growth and induction of *E. coli* XL1-Blue cells (Stratagene) transformed either with pOPE-LL or pOPE-SL plasmids as well as isolation of periplasmic inclusion bodies and purification of recombinant protein by IMAC under denaturing conditions were performed essentially as described (Kipriyanov *et al.*, 1996b). After IMAC, the eluted protein was reduced with 0.3 M DTE for two hours at ambient temperature and the four-domain single chain molecules were refolded by step-wise dialysis in presence of oxidized glutathione as described (Tsumoto *et al.*, 1998).

For long-time storage, antibody preparations were frozen in the presence of 2% human serum albumin (Immuno GmbH, Heidelberg, Germany) and stored at -80°C .

Measurement of protein concentration

The concentrations of purified scFv, diabody, sc-diabody and SL-Tandab were determined from the $A_{280 \text{ nm}}$ values using the extinction coefficients $\epsilon^{1 \text{ mg/ml}} = 1.84, 1.89, 1.93$ and 1.96 , respectively, calculated as described by Gill & von Hippel (1989).

Flow cytometry

The human CD3⁺/CD19[−] acute T cell leukemia line Jurkat and the CD19⁺/CD3[−] B cell line JOK-1 were used for flow cytometry as described (Kipriyanov *et al.*, 1998).

Affinity determination

The apparent affinities of the bispecific molecules were determined from competitive inhibition assays as previously described (Kipriyanov *et al.*, 1997b, 1998). Briefly, increasing concentrations of purified antibody fragment were added to a subsaturating concentration of FITC-labeled MAb OKT3 (anti-CD3) or HD37 (anti-CD19) and were incubated with Jurkat or JOK-1 cells, respectively. Fluorescence intensities of stained cells were measured using a FACScan flow cytometer (Becton Dickinson, Mountain View, CA). Binding affinities were calculated according to the following equation (Schodin & Kranz, 1993): $K_{D(I)} = IC_{50} / (1 + [\text{FITC-MAb}] / K_{D(\text{MAb})})$, where I is the unlabeled inhibitor (diabody, sc-diabody or Tandab), $[\text{FITC-MAb}]$ is the concentration of FITC-labeled MAb, $K_{D(\text{MAb})}$ is the binding affinity of MAb and IC_{50} is the concentration of inhibitor that yields 50% inhibition of binding. Affinity constant (K_D) values of 0.8 and 0.4 nM were assigned to MAb OKT3 (Adair *et al.*, 1994) and HD37 (Kipriyanov *et al.*, 1998), respectively.

In vitro cell surface retention

Cell surface retention assays were performed at 37°C essentially as described (Adams *et al.*, 1998) except that the detection of the retained antibody fragments was performed using anti-*c-myc* MAb 9E10 (IC Chemikalien) followed by FITC-labeled anti-mouse IgG. Kinetic dissociation constants (k_{off}) were calculated using a first order equation $F_t = F_0 e^{-kt}$, where F_t is a fluorescence at time t , F_0 is a fluorescence at time 0 and k is k_{off} . The half-life ($t_{1/2}$) for dissociation of antibody fragments was calculated from the equation $t_{1/2} = \ln 2 / k_{\text{off}}$.

Cell proliferation assay

Human PBL (1×10^4 /well) were cultured together with irradiated (120 rad) CD19⁺ Burkitt's lymphoma Raji cells (2.5×10^5 /well) in 96-well plate for five days in IMEM (Sigma, Deisenhofen, Germany) supplemented with 10% human AB serum (Sigma), 25 units/ml of recombinant human IL-2 (Chiron Corp., Emeryville, CA) and varying amounts of antibody fragments. ^3H -thymidine (0.5 μCi /well) was added 12 hours prior to harvesting. The cells were harvested and ^3H -thymidine incorporation was measured with a liquid scintillation beta-counter (Beckman, Palo Alto, CA).

Cytotoxicity assay

The efficacy of the BsAbs for mediating tumor cell lysis by activated human PBLs was determined using the JAM test (Matzinger, 1991). Briefly, 2.5×10^5

activated human PBLs prepared as described (Kipriyanov *et al.*, 1998), were mixed in round-bottomed microtiter plates with 1×10^4 of Raji cells labeled with [^3H]-thymidine (effector:target ratio = 25:1) in 100 μl medium plus 50 μl of antibody sample. After incubating the plate at 37°C , 5% CO_2 for four hours, the cells were harvested and radioactivity was measured with a liquid scintillation beta counter. Each experiment was carried out in triplicate. Specific killing (%) was calculated as (Matzinger, 1991): $(S-E)/S \times 100$, where E is experimentally retained labeled DNA in the presence of killers (in cpm) and S is retained DNA in the absence of killers (spontaneous).

Analyses of antibody stability *in vitro*

The antibody fragments were diluted (at least 20-fold) in human serum (Sigma) to a concentration of 15 $\mu\text{g}/\text{ml}$ and sterilized by filtration through a Membrex 4CA filter with a void volume of 50 μl and a pore size 0.2 μm (MembraPure, Lörzweiler, Germany). Aliquots (100 μl) were prepared at once under sterile conditions and stored at 37°C . At given time points, the aliquots were frozen and kept at -80°C . Activities of the samples after storage were determined by flow cytometry using CD3⁺ Jurkat cells. Protein degradation in each sample was determined by SDS-12% PAGE followed by Western blot analysis using anti-c-myc MAb 9E10 as described (Kipriyanov *et al.*, 1994).

Radioiodination

Antibody solutions (1 mg/ml in 50 mM Tris-HCl, 1 M NaCl, pH 7.0) were placed in glass tubes coated with 20 μg of IODO-Gen (Pierce, Rockford, IL) per mg of protein. After adding 3 mCi of [^{125}I]iodide (Amersham Buchler, Braunschweig, Germany), the resulting mixture was incubated for ten minutes at room temperature. Unincorporated radioiodine was separated from the labeled protein by size-exclusion chromatography using Bio-Gel P6 (Bio-Rad, Munich, Germany) and PBSI as the elution buffer. The final specific activities of scFv, diabody, LL and SL-Tandab were 2.4, 6.6, 4.0 and 3.8 mCi/mg, respectively.

Pharmacokinetic studies

Male NMRI mice each weighing approximately 40 g (24-27 animals for each labeled protein) were injected into the tail vein with 200 μl of PBSI containing 10 μg of human serum albumin and 5 μg of labeled antibody fragments. At the indicated time points, animals in triplicates were anaesthetized, bled and sacrificed in accordance with local animal protection laws. For scFv, the blood samples were obtained at 5, 10, 20, 40, 90, 180, 360 and 1080 minutes after injection. The time points for the diabody and tandem diabodies were the same, except that the last animal groups were sacrificed 24 hours after injection of the labeled compounds. Blood samples were counted using a gamma counter. Blood content was corrected for protein bound radioactivity (see below) and expressed as a percentage of injected dose per gram of blood (%ID/g). AUC was calculated using GraphPad Prism (GraphPad Software, San Diego, CA) and expressed as %ID/g per minute. The $t_{1/2\alpha}$ was defined by time points 5, 10, 20 and 40 minutes, while the $t_{1/2\beta}$ was defined by time points from 1.5 to 24 hours.

Analyses of antibody stability *in vivo*

A 200 μl sample of blood from each sacrificed animal mixed with 10 μl of heparin (5000 units/ml; Braun Melsungen AG, Melsungen, Germany) followed by sedimentation of cellular material and TCA precipitation of the supernatant. Radioactivity associated with pellets and supernatants was counted and expressed as a percentage of total radioactivity (cpm) for each specific time point. Pooled plasma samples from the earlier time points (up to 1.5 hours) were also analyzed by SDS-12% PAGE followed by autoradiography.

References

- Adair, J. R., Athwal, D. S., Bodmer, M., Bright, S. M., Collins, A., Pulito, V. L., Rao, P. E., Reedman, R., Rothermel, A. L., Xu, D., Zivin, R. A. & Jolliffe, L. K. (1994). Humanization of the murine anti-human CD3 monoclonal antibody OKT3. *Human Antibodies Hybrid.* 5, 41-47.
- Adams, G. P. (1998). Improving the tumor specificity and retention of antibody-based molecules. *In Vivo*, 12, 11-21.
- Adams, G. P., Schier, R., Marshall, K., Wolf, E. J., McCall, A. M., Marks, J. D. & Weiner, L. M. (1998). Increased affinity leads to improved selective tumor delivery of single-chain Fv antibodies. *Cancer Res.* 58, 485-490.
- Arakawa, T. & Timasheff, S. N. (1985). The stabilization of proteins by osmolytes. *Biophys. J.* 47, 411-414.
- Arndt, K. M., Müller, K. M. & Plückthun, A. (1998). Factors influencing the dimer to monomer transition of an antibody single-chain Fv fragment. *Biochemistry*, 37, 12918-12926.
- Arndt, M., Krauss, J., Kipriyanov, S. M., Pfreundschuh, M. & Little, M. (1999). A bispecific diabody that mediates natural killer cell cytotoxicity against xenotransplanted human Hodgkin's tumors. *Blood*, 94, 2562-2568.
- Bennett, M. J., Choe, S. & Eisenberg, D. (1994). Domain swapping: entangling alliances between proteins. *Proc. Natl Acad. Sci. USA*, 91, 3127-3131.
- Blackwell, J. R. & Horgan, R. (1991). A novel strategy for production of a highly expressed recombinant protein in an active form. *FEBS Letters*, 295, 10-12.
- Bohlen, H., Hopff, T., Manzke, O., Engert, A., Kube, D., Wickramanayake, P. D., Diehl, V. & Tesch, H. (1993). Lysis of malignant B cells from patients with B-chronic lymphocytic leukemia by autologous T cells activated with CD3 \times CD19 bispecific antibodies in combination with bivalent CD28 antibodies. *Blood*, 82, 1803-1812.
- Bothmann, H. & Plückthun, A. (1998). Selection for a periplasmic factor improving phage display and functional periplasmic expression. *Nature Biotechnol.* 16, 376-380.
- Bowden, G. A. & Georgiou, G. (1990). Folding and aggregation of beta-lactamase in the periplasmic space of *Escherichia coli*. *J. Biol. Chem.* 265, 16760-16766.
- Brennan, M., Davidson, P. F. & Paulus, H. (1985). Preparation of bispecific antibodies by chemical recombination of monoclonal immunoglobulin G1 fragments. *Science*, 229, 81-83.
- Carter, P., Ridgway, J. & Zhu, Z. (1995). Toward the production of bispecific antibody fragments for clinical applications. *J. Hematother.* 4, 463-470.

- Casey, J. L., Keep, P. A., Chester, K. A., Robson, L., Hawkins, R. E. & Begent, R. H. (1995). Purification of bacterially expressed single chain Fv antibodies for clinical applications using metal chelate chromatography. *J. Immunol. Methods*, **179**, 105-116.
- Coloma, M. J. & Morrison, S. L. (1997). Design and production of novel tetravalent bispecific antibodies. *Nature Biotechnol.* **15**, 159-163.
- de Kruif, J. & Logtenberg, T. (1996). Leucine zipper dimerized bivalent and bispecific scFv antibodies from a semi-synthetic antibody phage display library. *J. Biol. Chem.* **271**, 7630-7634.
- Fanger, M. W., Morganelli, P. M. & Guyre, P. M. (1992). Bispecific antibodies. *Crit. Rev. Immunol.* **12**, 101-124.
- FitzGerald, K., Holliger, P. & Winter, G. (1997). Improved tumour targeting by disulphide stabilized diabodies expressed in *Pichia pastoris*. *Protein Eng.* **10**, 1221-1225.
- Gill, S. C. & von Hippel, P. H. (1989). Calculation of protein extinction coefficients from amino acid sequence data. *Anal. Biochem.* **182**, 319-326.
- Givol, D. (1991). The minimal antigen-binding fragment of antibodies-Fv fragment. *Mol. Immunol.* **28**, 1379-1386.
- Glennie, M. J., McBride, H. M., Worth, A. T. & Stevenson, G. T. (1987). Preparation and performance of bispecific F(ab')₂ antibody containing thioether-linked Fab'γ fragments. *J. Immunol.* **139**, 2367-2375.
- Glockshuber, R., Malia, M., Pfitzinger, I. & Plückthun, A. (1990). A comparison of strategies to stabilize immunoglobulin Fv-fragments. *Biochemistry*, **29**, 1362-1367.
- Gruber, M., Schodin, B. A., Wilson, E. R. & Kranz, D. M. (1994). Efficient tumor cell lysis mediated by a bispecific single chain antibody expressed in *Escherichia coli*. *J. Immunol.* **152**, 5368-5374.
- Harris, L. J., Skaletsky, E. & McPherson, A. (1998). Crystallographic structure of an intact IgG1 monoclonal antibody. *J. Mol. Biol.* **275**, 861-872.
- Holck, A. & Kleppe, K. (1988). Cloning and sequencing of the gene for the DNA-binding 17 K protein of *Escherichia coli*. *Gene*, **67**, 117-124.
- Holliger, P., Prospero, T. & Winter, G. (1993). "Diabodies": small bivalent and bispecific antibody fragments. *Proc. Natl Acad. Sci. USA*, **90**, 6444-6448.
- Holliger, P., Brissinck, J., Williams, R. L., Thielemans, K. & Winter, G. (1996). Specific killing of lymphoma cells by cytotoxic T-cells mediated by a bispecific diabody. *Protein Eng.* **9**, 299-305.
- Horn, U., Strittmatter, W., Krebber, A., Knupfer, U., Kujau, M., Wenderoth, R., Müller, K., Matzku, S., Plückthun, A. & Riesenberg, D. (1996). High volumetric yields of functional dimeric miniantibodies in *Escherichia coli*, using an optimized expression vector and high-cell-density fermentation under non-limited growth conditions. *Appl. Microbiol. Biotechnol.* **46**, 524-532.
- Huston, J. S., Levinson, D., Mudgett, Hunter M., Tai, M. S., Novotny, J., Margolies, M. N., Ridge, R. J., Brucoleri, R. E., Haber, E., Crea, R. & Oppermann, H. (1988). Protein engineering of antibody binding sites: recovery of specific activity in an anti-digoxin single-chain Fv analogue produced in *Escherichia coli*. *Proc. Natl Acad. Sci. USA*, **85**, 5879-5883.
- Khazaali, M. B., Conry, R. M. & LoBuglio, A. F. (1994). Human immune response to monoclonal antibodies. *J. Immunother.* **15**, 42-52.
- Kipriyanov, S. M., Dübel, S., Breitling, F., Kontermann, R. E. & Little, M. (1994). Recombinant single-chain Fv fragments carrying C-terminal cysteine residues: production of bivalent and biotinylated miniantibodies. *Mol. Immunol.* **31**, 1047-1058.
- Kipriyanov, S. M., Kupriyanova, O. A., Little, M. & Moldenhauer, G. (1996a). Rapid detection of recombinant antibody fragments directed against cell-surface antigens by flow cytometry. *J. Immunol. Methods*, **196**, 51-62.
- Kipriyanov, S. M., Little, M., Kropshofer, H., Breitling, F., Gotter, S. & Dübel, S. (1996b). Affinity enhancement of a recombinant antibody: formation of complexes with multiple valency by a single-chain Fv fragment-core streptavidin fusion. *Protein Eng.* **9**, 203-211.
- Kipriyanov, S. M., Moldenhauer, G. & Little, M. (1997a). High level production of soluble single chain antibodies in small-scale *Escherichia coli* cultures. *J. Immunol. Methods*, **200**, 69-77.
- Kipriyanov, S. M., Moldenhauer, G., Martin, A. C., Kupriyanova, O. A. & Little, M. (1997b). Two amino acid mutations in an anti-human CD3 single chain Fv antibody fragment that affect the yield on bacterial secretion but not the affinity. *Protein Eng.* **10**, 445-453.
- Kipriyanov, S. M., Moldenhauer, G., Strauss, G. & Little, M. (1998). Bispecific CD3 × CD19 diabody for T cell-mediated lysis of malignant human B cells. *Int. J. Cancer*, **77**, 763-772.
- Kung, P. C., Golstein, G., Reinherz, E. L. & Schlossman, S. F. (1979). Monoclonal antibodies defining distinctive human T cell surface antigens. *Science*, **206**, 347-349.
- Kurucz, I., Titus, J. A., Jost, C. R., Jacobus, C. M. & Segal, D. M. (1995). Retargeting of CTL by an efficiently refolded bispecific single-chain Fv dimer produced in bacteria. *J. Immunol.* **154**, 4576-4582.
- Lee, J. C. & Timasheff, S. N. (1981). The stabilization of proteins by sucrose. *J. Biol. Chem.* **256**, 7193-7201.
- Le, Gall F., Kipriyanov, S. M., Moldenhauer, G. & Little, M. (1999). Di-, tri- and tetrameric single chain Fv antibody fragments against human CD19: effect of valency on cell binding. *FEBS Letters*, **453**, 164-168.
- Mallender, W. D., Carrero, J. & Voss, E. (1996). Comparative properties of the single chain antibody and Fv derivatives of mAb 4-4-20. Relationship between interdomain interactions and the high affinity for fluorescein ligand. *J. Biol. Chem.* **271**, 5338-5346.
- Matzinger, P. (1991). The JAM test. A simple assay for DNA fragmentation and cell death. *J. Immunol. Methods*, **145**, 185-192.
- Maurer, R., Meyer, B. & Ptashne, M. (1980). Gene regulation at the right operator (O_R) bacteriophage λ. I. O_R3 and autogenous negative control by repressor. *J. Mol. Biol.* **139**, 147-161.
- Müller, K. M., Arndt, K. M., Bauer, K. & Plückthun, A. (1998a). Tandem immobilized metal-ion affinity chromatography/immunoaffinity purification of His-tagged proteins-evaluation of two anti-His-tag monoclonal antibodies. *Anal. Biochem.* **259**, 54-61.
- Müller, K. M., Arndt, K. M. & Plückthun, A. (1998b). A dimeric bispecific miniantibody combines two specificities with avidity. *FEBS Letters*, **432**, 45-49.
- Müller, K. M., Arndt, K. M., Strittmatter, W. & Plückthun, A. (1998c). The first constant domain (C_{H1} and C_L) of an antibody used as heterodimerization domain for bispecific miniantibodies. *FEBS Letters*, **422**, 259-264.

- Nieba, L., Honegger, A., Krebber, C. & Plückthun, A. (1997). Disrupting the hydrophobic patches at the antibody variable/constant domain interface: improved *in vivo* folding and physical characterization of an engineered scFv fragment. *Protein Eng.* **10**, 435-444.
- Perisic, O., Webb, P. A., Holliger, P., Winter, G. & Williams, R. L. (1994). Crystal structure of a diabody, a bivalent antibody fragment. *Structure*, **2**, 1217-1226.
- Pezzutto, A., Dörken, B., Rabinovitch, P. S., Ledbetter, J. A., Moldenhauer, G. & Clark, E. A. (1987). CD19 monoclonal antibody HD37 inhibits anti-immunoglobulin-induced B cell activation and proliferation. *J. Immunol.* **138**, 2793-2799.
- Plückthun, A. & Pack, P. (1997). New protein engineering approaches to multivalent and bispecific antibody fragments. *Immunotechnology*, **3**, 83-105.
- Polymenis, M. & Stollar, B. D. (1995). Domain interactions and antigen binding of recombinant anti-Z-DNA antibody variable domains. The role of heavy and light chains measured by surface plasmon resonance. *J. Immunol.* **154**, 2198-2208.
- Ridder, R., Schmitz, R., Legay, F. & Gram, H. (1995). Generation of rabbit monoclonal antibody fragments from a combinatorial phage display library and their production in the yeast *Pichia pastoris*. *Bio/Technology*, **13**, 255-260.
- Rodriguez, R., Chinea, G., Lopez, N., Pons, T. & Vriend, G. (1998). Homology modeling, model and software evaluation: three related resources. *Bioinformatics*, **14**, 523-528.
- Sanger, F., Nicklen, S. & Coulson, A. R. (1977). DNA sequencing with chain-terminating inhibitors. *Proc. Natl Acad. Sci. USA*, **74**, 5463-5467.
- Sawyer, J. R., Schlom, J. & Kashmiri, S. V. S. (1994). The effect of induction conditions on production of a soluble anti-tumor sFv in *Escherichia coli*. *Protein Eng.* **7**, 1401-1406.
- Schlunegger, M. P., Bennett, M. J. & Eisenberg, D. (1997). Oligomer formation by 3D domain swapping: a model for protein assembly and misassembly. *Advan. Protein Chem.* **50**, 61-122.
- Schodin, B. A. & Kranz, D. M. (1993). Binding affinity and inhibitory properties of a single-chain anti-T cell receptor antibody. *J. Biol. Chem.* **268**, 25722-25727.
- Schulze, R. A., Kontermann, R. E., Queitsch, I., Dübel, S. & Bautz, E. K. (1994). Thiophilic adsorption chromatography of recombinant single-chain antibody fragments. *Anal. Biochem.* **220**, 212-214.
- Shusta, E. V., Raines, R. T., Plückthun, A. & Wittrup, K. D. (1998). Increasing the secretory capacity of *Saccharomyces cerevisiae* for production of single-chain antibody fragments. *Nature Biotechnol.* **16**, 773-777.
- Thisted, T., Sorensen, N. S., Wagner, E. G. & Gerdes, K. (1994). Mechanism of post-segregational killing: Sok antisense RNA interacts with Hok mRNA via its 5'-end single-stranded leader and competes with the 3'-end of Hok mRNA for binding to the mok translational initiation region. *EMBO J.* **13**, 1960-1968.
- Tsumoto, K., Shinoki, K., Kondo, H., Uchikawa, M., Juji, T. & Kumagai, I. (1998). Highly efficient recovery of functional single-chain Fv fragments from inclusion bodies overexpressed in *Escherichia coli* by controlled introduction of oxidizing reagent-application to a human single-chain Fv fragment. *J. Immunol. Methods*, **219**, 119-129.
- Uckun, F. M. & Ledbetter, J. A. (1988). Immunobiologic differences between normal and leukemic human B-cell precursors. *Proc. Natl Acad. Sci. USA*, **85**, 8603-8607.
- Xie, G. & Timasheff, S. N. (1997). Mechanism of the stabilization of ribonuclease A by sorbitol: preferential hydration is greater for the denatured than for the native protein. *Protein Sci.* **6**, 211-221.
- Zhu, Z., Zapata, G., Shalaby, R., Snedecor, B., Chen, H. & Carter, P. (1996). High level secretion of a humanized bispecific diabody from *Escherichia coli*. *Bio/Technology*, **14**, 192-196.
- Zhu, Z., Presta, L. G., Zapata, G. & Carter, P. (1997). Remodeling domain interfaces to enhance heterodimer formation. *Protein Sci.* **6**, 781-788.

Edited by J. Karn

(Received 8 June 1999; received in revised form 1 September 1999; accepted 1 September 1999)